A Causal Role for the Hippocampus in Gating Rapid Motor Memory Consolidation

Maria Paz Montenegro[1], Shancheng Bao[1], Sapna Bisht[2], Kenneth L. Hoyt[2], Huiliang Wang[3], David L. Wright[1], John J. Buchanan[1], Yuming Lei[1]

[1]Program of Motor Neuroscience, Department of Kinesiology & Sport Management, Texas A&M University, College Station, TX, USA.

[2]Department of Biomedical Engineering, Texas A&M University, College Station, TX, USA.

[3]Department of Biomedical Engineering, Cockrell School of Engineering, The University of Texas at Austin, Austin, TX, USA.

Abbreviated title: Hippocampal Gating of Motor Consolidation
Number of figures: 6
Number of tables: 0
Number of pages: 43
Competing interests: The authors declare no competing interests.
Data availability statement: The data that support the findings of this study are available from the corresponding author upon reasonable request.
Keywords: Memory Consolidation, Hippocampus, Transcranial Ultrasound Stimulation, Neuromodulation, Motor Skill Learning, Neuroplasticity.

Abstract

How humans learn new skills is a fundamental aspect of behavior. Rapid memory consolidation during brief rests is crucial, but the causal role of the hippocampus remains unclear. Here, we used personalized transcranial ultrasound stimulation (TUS) to non-invasively modulate the hippocampus. We found that hippocampal neuromodulation fundamentally alters how a skill is learned. Compared to sham stimulation, TUS shifted performance gains from rest periods (offline consolidation) to active practice (online learning). Paradoxically, this manipulation not only reshaped the learning process but also boosted overall performance by unmasking a latent and highly efficient online learning pathway, leading to superior skill retention 24 hours later. These findings provide causal evidence that the hippocampus acts as a gating mechanism, governing a key trade-off between online and offline learning pathways. Our work demonstrates that non-invasive deep brain modulation can causally alter the balance between competing memory systems, opening new avenues to optimize human performance.

Keywords: Memory Consolidation, Hippocampus, Transcranial Ultrasound Stimulation, Neuromodulation, Motor Skill Learning, Neuroplasticity.

Introduction

The ability to learn motor skills through practice is fundamental to human achievement, from mastering daily routines to reaching the pinnacle of expert performance[1,2]. Central to this process is offline memory consolidation, during which fragile new memories are stabilized into more robust forms, resilient to decay and interference[3-9]. Beyond the well-established memory consolidation that unfolds over hours and often involves sleep[9-12], a growing body of evidence highlights a rapid form of consolidation operating on a timescale of seconds. This "micro-consolidation," occurring during brief rests interspersed with practice, powerfully shapes the initial stages of learning[13-15].

A convergence of evidence implicates the hippocampus as a key neural substrate for this rapid micro-consolidation. For instance, neuroimaging studies reveal that heightened hippocampal activity during these brief rests predicts subsequent 'micro-offline' performance gains[13-15], while the hippocampus also exhibits rapid structural and functional plasticity to support the learning of motor sequences[14]. Moreover, interventions that disrupt the integrity of the hippocampal networks - such as prefrontal stimulation that alters its reactivation[16] or direct hippocampal lesions[17] - impair these micro-offline benefits without affecting motor execution. While compelling, this evidence remains fundamentally indirect. Neuroimaging reveals correlation, not causation, while lesion and network disruption studies cannot isolate the hippocampus from the confounding effects of pathology or compensatory mechanisms. Thus, establishing a definitive causal link requires a tool capable of precise, reversible, and targeted neuromodulation of the hippocampus itself.

This demand for a targeted tool presents a profound challenge

for conventional technologies. Non-invasive techniques like transcranial magnetic stimulation (TMS) and transcranial electrical stimulation (tES) are fundamentally limited by poor spatial focality - on the order of centimeters - and insufficient penetration depth[18]. These limitations preclude the selective engagement of deep targets like the hippocampus without causing significant, off-target stimulation of the overlying cortex, thereby confounding any causal inference[19-21]. Conversely, while invasive methods such as deep brain stimulation (DBS) offer the necessary precision to target key structures within hippocampal circuits like the fornix[22-25], their application in healthy populations is precluded by significant safety risks, including hemorrhage and infection[26,27]. As a result, the causal role of deep brain structures in human cognition has remained largely inaccessible to direct investigation.

Transcranial ultrasound stimulation (TUS) is a transformative technology that bridges this methodological gap. TUS overcomes the limitations of prior methods by using acoustic energy to non-invasively modulate deep brain regions with millimeter-scale spatial accuracy - a profound leap in precision[28-31]. Its neuromodulatory effects are thought to arise from precisely controlled mechanical interactions between acoustic waves and neural tissue, which likely engage mechanosensitive ion channels to drive both transient and lasting changes in local neural activity[32,33]. This precise control over acoustic parameters also enables the induction of lasting neuroplastic effects, analogous to long-term potentiation or depression[34]. The safety and efficacy of TUS in modulating deep brain activity are now well-established across species, from rodents to non-human primates and humans[35-47]. Crucially for the present work, TUS directed at the hippocampus or its connected circuits has already been shown to modulate learning and

memory processes in both animals[48] and humans[49]. This established, targeted, and non-invasive capability thus positions TUS as the ideal tool to directly probe the causal contributions of the hippocampus to the rapid dynamics of memory consolidation in humans.

Here, we applied low-intensity TUS to directly test the causal role of the human hippocampus in rapid motor memory consolidation. Our approach involved several key validation and experimental stages. First, we conducted a thorough acoustic validation, using hydrophone measurements to confirm the accuracy of computational models, which were then used for personalized TUS targeting based on individual pseudo-CT images derived from each participant's MRI. Second, we confirmed the neuromodulatory efficacy of our TUS parameters by demonstrating their ability to induce a sustained suppression of cortical excitability in the primary motor cortex (M1), as assessed by motor-evoked potentials (MEPs). Finally, and crucially, we examined the behavioral impact of this personalized hippocampal TUS on motor sequence learning in healthy participants. We found that hippocampal TUS fundamentally reshapes the dynamics of rapid memory consolidation, shifting performance gains from offline rest to online practice and thereby abolishing micro-consolidation gains. Paradoxically, this disruption did not impair learning but rather enhanced it, significantly boosting initial performance and accelerating skill retention 24 hours later.

Results

We investigated the causal role of the hippocampus in rapid motor memory consolidation using a randomized, between-subject design in which participants received either active TUS targeted to the hippocampus or a sham stimulation before performing a motor sequence learning task on Day 1. As depicted in Fig. 1A, the main experiment consisted of 36 trials, followed by a 9-trial retention test approximately 24 hours later on Day 2. Each trial was composed of a 10-second practice period, where participants typed a five-element sequence, followed by a 10-second rest period. Our results are presented in three parts. We first detail the technical validation of our TUS protocol, then present the primary behavioral findings from Day 1, and finally, examine the lasting impact of the intervention on skill retention 24 hours later.

Ultrasound Field Characterization and Simulation Validation

To validate our acoustic simulation, we first physically characterized the acoustic output of the 0.5-MHz transducer using hydrophone measurements in a degassed water tank (Fig. 1B). The physical measurements and simulation showed excellent concordance, as demonstrated by the strong overlap between the measured (red) and simulated (blue) axial pressure profiles (Fig. 1C). The measured focal depth was 111.4 mm, closely matching the simulation's target of 112.0 mm, which represents the average depth required to target the posterior hippocampus. At a target spatial-peak pulse-average intensity (I_{sppa}) of 35 W/cm², the measured peak pressure was 1.03 MPa, in strong agreement with the simulated value of 1.02 MPa. This high degree of agreement confirms the fidelity of the acoustic simulation model. With the simulation thus validated, we used it to characterize the three-dimensional pressure field (Fig. 1D). The simulation revealed

152 a highly collimated acoustic wave resulting in an elongated, ellipsoidal focal spot. The
153 axial full-width at half-maximum (FWHM) was 62.7 mm, with a -6 dB width of 94.1 mm. In
154 contrast, the focus was highly confined in the lateral plane, with a FWHM of just 5.3
155 mm and a -6 dB width of 7.3 mm (Fig. 1D, right panels). Together, these measurements
156 and validated simulations verify our protocol's capacity to generate a highly localized
157 acoustic focus, making it suitable for spatially precise targeting of deep brain structures
158 due to its millimeter-scale lateral resolution.

159 **Personalized TUS Targeting Using Transcranial Acoustic Simulations**

160 To ensure precise and safe delivery of acoustic energy to the hippocampus, we employed
161 a personalized TUS targeting pipeline for each participant. This process involved
162 acquiring a high-resolution T1-weighted anatomical MRI (Fig. 2A, top row) to generate a
163 subject-specific pseudo-CT, which provided a detailed model of individual skull density
164 and morphology for acoustic simulation (Fig. 2A, middle row). These individual models
165 enabled transcranial acoustic simulations to optimize transducer placement and map the
166 resulting pressure field, confirming that the acoustic focus could be reliably steered onto
167 the hippocampus, as demonstrated for a representative participant (Fig. 2A, bottom row).
168 Across all participants, the mean transducer focal depth was 112.0 ± 6.3 mm with a
169 spatial-peak pulse-average intensity (I_{sppa}) of 35.9 ± 7.7 W/cm². After accounting for skull
170 attenuation, the simulations predicted a mean in situ I_{sppa} at the hippocampus of 4.3 ±
171 0.06 W/cm² and a corresponding pressure of 0.36 ± 0.003 MPa. Crucially, the simulations
172 confirmed the protocol's safety for both mechanical and thermal effects. The
173 predicted mechanical index (MI) was 0.52 ± 0.03, well below the FDA's mechanical safety
174 limit. The predicted thermal dose (CEM43) was negligible ($3.88 \times 10^{-4} \pm 2.7 \times 10^{-6}$),

175 indicating a minimal risk of tissue heating. This individualized procedure is critical for
176 ensuring that neuromodulatory effects are confined to the target region, validating our
177 ability to causally probe the function of this deep brain structure with high anatomical
178 fidelity.

179 **TUS Protocol Induces Sustained Suppression of Motor Cortex Excitability**

180 To first validate the neuromodulatory efficacy of our TUS protocol, we quantified its effect
181 on primary motor cortex (M1) excitability. We measured motor-evoked potentials (MEPs)
182 elicited by single-pulse TMS at baseline, and again at 5 and 30 minutes following either
183 active TUS or a sham procedure over M1. A mixed-model ANOVA revealed a significant
184 interaction between TUS condition and Time ($F_{(2, 76)} = 4.218$, $p = 0.02$), confirming that
185 active TUS modulated cortical excitability differently than sham stimulation over time.
186 Post-hoc analysis of the active TUS condition confirmed a robust and sustained
187 suppression of MEP amplitude (Fig. 2C), an effect that was also apparent in
188 representative single-subject data (Fig. 2B). Specifically, MEPs were significantly
189 reduced from a baseline of 1.15 ± 0.30 mV to 0.92 ± 0.30 mV at 5 minutes ($p = 0.004$)
190 and remained suppressed at 0.96 ± 0.29 mV at 30 minutes ($p = 0.01$). In contrast, MEP
191 amplitudes in the sham condition remained stable across all time points (Fig. 2D), with no
192 significant changes from baseline (1.16 ± 0.58 mV) at either 5 minutes (1.22 ± 0.65 mV;
193 $p = 0.5$) or 30 minutes (1.24 ± 0.67 mV; $p = 0.2$). These results confirm that our TUS
194 protocol produces a sustained inhibitory effect on cortical excitability lasting at least 30
195 minutes. Crucially, this duration confirms that the intended neuroinhibitory state was
196 maintained throughout the entire duration of the main behavioral experiment, thereby
197 validating the protocol's efficacy for testing the causal role of hippocampal inhibition.

198 **Hippocampal TUS Alters the Dynamics of Rapid Memory Consolidation**

199 To investigate how hippocampal TUS affected the learning process, we dissected
200 performance data from Day 1 into two components, following the methodology of prior
201 work on rapid consolidation[13]. "Micro-online gains" were defined as the change in tapping
202 speed from the first to the last correct sequence within a 10-s practice period, while
203 "micro-offline gains" were defined as the change in tapping speed from the last correct
204 sequence of one trial to the first correct sequence of the next (Fig. 3A and D). First, we
205 examined the sham stimulation group to establish the baseline learning pattern.
206 Consistent with previous findings, we found that skill acquisition was driven exclusively
207 by improvements occurring during brief rests. This pattern was apparent on a trial-by-trial
208 basis, where micro-offline gains were consistently positive while micro-online gains
209 fluctuated around zero (Fig. 3B). Analysis of the summed gains (Fig. 3C) confirmed that
210 learning was driven by micro-offline consolidation. The total micro-offline gains were
211 significantly positive ($t(19) = 2.627$, $p = 0.02$), whereas the total micro-online gains did not
212 significantly differ from zero ($t(19) = -1.523$, $p = 0.14$).

213 In contrast, applying inhibitory TUS to the hippocampus fundamentally reversed
214 this learning dynamic, shifting the source of performance improvements from rest to
215 active practice (Fig. 3E). Analysis of the summed gains (Fig. 3F) confirmed that learning
216 was now driven by micro-online practice, as the total micro-online gains were significantly
217 positive ($t(19) = 2.245$, $p = 0.03$). Conversely, the offline consolidation observed in the
218 sham group was abolished. The total micro-offline gains did not significantly differ from
219 zero ($t(19) = -1.504$, $p = 0.15$). This dissociation in learning strategies was confirmed by
220 a direct statistical comparison between the groups (Fig. 3G). The hippocampal TUS group

exhibited significantly greater micro-online gains than the sham group ($t(38) = 2.709$, $p = 0.010$). Conversely, the sham group exhibited significantly greater micro-offline gains than the TUS group ($t(38) = -2.743$, $p = 0.009$). This clear dissociation confirms that hippocampal TUS fundamentally shifted the source of performance improvements from offline rest to online practice.

Despite these divergent dynamics, we observed a consistent underlying principle governing both learning modes. A strong negative correlation emerged between the total micro-online and micro-offline gains for all participants, revealing a direct trade-off between improvements made during practice versus rest ($R^2 > 0.98$, $p < 0.001$ for both groups; Fig. 3H). Hippocampal TUS did not eliminate this fundamental trade-off but instead shifted participants along its spectrum. Sham participants clustered in a "low-online / high-offline" regime consistent with a consolidation-dominant strategy. In contrast, the TUS group occupied a distinct "high-online / low-offline" regime. This finding reveals that while the online-offline trade-off is a conserved feature of motor learning, hippocampal TUS causally biases this process toward immediate gains during active practice.

Hippocampal TUS Overcomes Performance Plateaus

The altered learning dynamics in the TUS group resulted in superior overall task performance, as illustrated by the group-averaged learning curves (Fig. 4A). This superiority was established by an immediate performance boost, rather than an accelerated rate of learning. Indeed, the sham group exhibited a significantly faster learning rate ($t(38) = 2.124$, $p = 0.040$; Fig. 4B). To test whether this performance advantage was sustained, we compared the average tapping speed between groups after

each participant had reached their performance plateau (95% of total learning). This analysis confirmed a lasting benefit, as the TUS group was significantly faster than the sham group during this plateau phase ($t(38) = -2.166$, $p = 0.037$; Fig. 4C). This result indicates that the TUS group was more resistant to the performance ceilings that typically emerge with extended practice, suggesting that by promoting continuous online gains, hippocampal TUS helps to counteract performance plateaus.

Altered Learning Dynamics and Superior Performance Persist 24 Hours Later

To determine if the TUS-induced changes were lasting, we tested participants again on Day 2. The results reveal a remarkable persistence of the TUS-induced effects, with the stimulation group retaining its distinct learning strategy and its performance advantage. During the relearning session, the sham group's performance had plateaued, with neither the sum of micro-online gains ($p = 0.06$) nor micro-offline gains ($p = 0.6$) differing significantly from zero (Fig. 5A-C). In stark contrast, the TUS group continued to exhibit a robust practice-based learning pattern (Fig. 5D, E). Relearning was driven exclusively by highly significant micro-online gains ($t(19) = 5.892$, $p < 0.001$), and was accompanied by a significant performance decay during rest periods, as the sum of micro-offline gains was significantly negative ($t(19) = -5.070$, $p < 0.001$; Fig. 5F). This lasting mechanistic divergence translated directly into superior overall task performance, with the TUS group maintaining a significantly higher tapping speed throughout the entire Day 2 relearning session ($t(38) = -2.246$, $p = 0.031$; Fig. 5G). Direct statistical comparisons confirmed these differences, showing the TUS group achieved significantly greater micro-online gains ($p < 0.001$; Fig. 5H), while the sham group showed significantly greater micro-offline gains ($p < 0.001$; Fig. 5I). These results demonstrate that a single session of hippocampal

TUS induced a durable change in the neural mechanisms of skill relearning, conferring a sustained performance advantage 24 hours later.

Hippocampal TUS Disrupts the Link Between Rapid and Overnight Consolidation

We next investigated how the distinct learning dynamics observed on Day 1 predicted the magnitude of offline consolidation that occurred overnight. We quantified this overnight consolidation by calculating the change in performance from the last trial of Day 1 to the first trial of Day 2 (Fig. 6A). Overall, both the sham group ($t(19) = -0.399$, $p = 0.7$) and the TUS group ($t(19) = -0.984$, $p = 0.3$) showed no significant net change in performance overnight, and there was no significant difference in overnight gains between the groups ($p = 0.6$; Fig. 6B). However, a strong predictive relationship emerged between the type of learning on Day 1 and the magnitude of these overnight gains in the sham group. The sum of micro-offline gains on Day 1 was significantly and positively correlated with overnight consolidation ($p = 0.027$; Fig. 6C), indicating that participants who consolidated more effectively during brief rests also consolidated more during sleep. Conversely, the sum of micro-online gains was significantly negatively correlated with overnight gains ($p = 0.022$; Fig. 6D). This pattern suggests that under normal conditions, a consistent consolidation-based mechanism is engaged during both short rests and overnight sleep. In contrast, this entire predictive relationship was completely abolished in the hippocampal TUS group. Neither the sum of micro-offline gains ($p = 0.740$; Fig. 6E) nor the sum of micro-online gains ($p = 0.957$; Fig. 6F) showed any significant correlation with the change in performance overnight. This dissociation indicates that hippocampal TUS fundamentally disrupted the normal link between the mechanisms of rapid, within-session consolidation and subsequent, overnight memory stabilization.

Discussion

Our study provides the first causal evidence that the human hippocampus is a key contributor in the rapid consolidation of motor memories, actively gating whether learning gains occur during active practice or during periods of rest. By applying non-invasive transcranial ultrasound stimulation (TUS) to the hippocampus, we fundamentally altered the process of skill acquisition, shifting its primary mechanism from offline micro-consolidation during brief rests to online learning during active practice. Crucially, this TUS-induced shift from an offline to an online learning mode was not merely a redistribution of learning but paradoxically enhanced the overall magnitude of skill acquisition. These findings causally establish the hippocampus's role in governing the trade-off between online and offline learning pathways, demonstrating that this function can be non-invasively modulated to reshape human skill acquisition.

The most striking finding of this study was the TUS-induced reversal of learning dynamics from a micro-offline to a micro-online mode. Our sham group robustly replicated the well-established "micro-consolidation" phenomenon[13], where performance improvements emerge almost exclusively during brief rest periods. This process is thought to be supported by the reactivation of learning-related neural patterns, with neuroimaging studies showing that waking hippocampo-neocortical replay and activity during rest are predictive of these behavioral gains[14,15]. Furthermore, studies of amnesic patients with hippocampal damage and those using network disruption via prefrontal stimulation both demonstrate that interfering with hippocampal function impairs or hinders these offline gains[16,17]. While our findings confirm the hippocampus's causal role, they also provide a critical new insight into its specific function. Direct TUS inhibition of the

hippocampus abolished offline gains and forced learning to occur exclusively during active practice. This provides a more nuanced view than that offered by previous lesion and network disruption studies. While those approaches establish that the hippocampus is necessary for offline consolidation, our use of direct, reversible modulation suggests it also acts as a powerful gating mechanism. It appears to actively enforce an "offline-first" strategy, suppressing concurrent online learning in favor of rest-based consolidation. Thus, our work demonstrates that the hippocampus does not merely support consolidation but actively orchestrates its timing, revealing a new layer of control in the dynamics of rapid motor skill learning.

We propose that by inhibiting this hippocampal gating mechanism, the TUS intervention effectively released a "brake" on corticostriatal circuits, allowing these structures to engage in rapid, online error correction and stabilization. This interpretation is grounded in the well-established theory of competitive memory systems, which posits a functional trade-off between the hippocampal declarative system and the striatal procedural system[50]. A body of evidence demonstrates that compromising one system can, in some cases, enhance the function of the other. For instance, in rodents, dorsal hippocampal lesions paradoxically boost performance in a sequential reaction time task[51]. A similar principle has been observed in humans, where amnesic patients with hippocampal damage can show superior implicit learning on sequence tasks compared to controls[52]. Furthermore, placing the declarative system under cognitive load in healthy individuals biases the brain toward the striatal habit system and improves performance on probabilistic learning tasks[53]. Our intervention most likely biased this competitive balance in a similar manner, disinhibiting the corticostriatal system responsible for online,

practice-dependent skill acquisition.

Our results reveal a strong negative correlation between total micro-online and micro-offline gains across all participants, suggesting these two modes of improvement operate in a zero-sum trade-off. This finding has significant theoretical implications, suggesting a finite capacity for within-session improvement that can be allocated to either rest or practice, but not maximally to both. In the sham group, the brain's default strategy clustered in the "low-online / high-offline" regime. This likely represents an optimized state that prioritizes memory stability, as offline consolidation driven by hippocampo-neocortical replay is thought to protect the neocortex from "catastrophic interference"—a form of rapid, unstable learning that can overwrite existing memories[54]. Conversely, the TUS group occupied a "high-online / low-offline" regime. The fact that this group achieved superior overall performance suggests that the online, practice-dependent pathway—likely mediated by corticostriatal circuits known to be critical for procedural skill acquisition[55]—is inherently more potent for this specific task. The hippocampus, therefore, may act as a rate-limiting bottleneck in the early stages of skill acquisition. By enforcing an "offline-first" consolidation strategy, it may prevent the motor system from achieving its maximum potential rate of improvement. By inhibiting this hippocampal gate, TUS appears to have unmasked a state of enhanced performance where these gains were realized immediately.

Our findings also challenge the conventional understanding of the relationship between rapid (waking) and long-term (sleep-dependent) consolidation. A prevailing serial model suggests that neural reactivation during brief rests acts as a precursor, "tagging" memories for more extensive replay during slow-wave sleep, which is critical for

long-term retention[9,56]. Consistent with this model, our sham group demonstrated that participants who consolidated more effectively during brief rests also showed greater gains overnight, supporting the idea that waking consolidation is a prerequisite for subsequent sleep-dependent stabilization. In contrast, this relationship was completely disrupted by the TUS intervention. In the stimulation group, the magnitude of Day 1 learning (primarily driven by online gains) had no relationship to overnight changes. Crucially, however, the TUS group still retained its superior performance on Day 2. This demonstrates that memories formed via the "online" pathway were robust and stable over 24 hours, even without the apparent prerequisite of micro-offline consolidation. This result directly challenges a strict serial model of memory consolidation, in which information must pass sequentially from hippocampal encoding to waking replay and then to sleep-dependent processes[57]. Instead, our findings provide strong support for a parallel processing model of motor memory, suggesting that the online mechanism, likely centered in striato-cortical loops, can create stable, lasting motor engrams independently of the classic hippocampal offline consolidation machinery. This has significant implications for our understanding of memory, suggesting the canonical hippocampal-dependent consolidation pathway is just one of several potentially redundant and interacting mechanisms available to the human brain[58,59].

It is important to acknowledge that the interpretation of micro-offline gains as a direct measure of memory consolidation is a subject of ongoing debate. A recent series of behavioral experiments argued that these gains do not reflect true offline learning but rather transient performance benefits arising from recovery from fatigue and motor pre-planning. However, two key findings from our study are difficult to reconcile with an

interpretation based solely on non-memory-related factors. First, an explanation based on peripheral motor fatigue or generic planning cannot easily account for the fact that targeted inhibition of the hippocampus specifically abolished these improvements. Second, if micro-offline gains were merely a transient benefit, their abolition in our TUS group should not have led to a paradoxical enhancement of overall skill acquisition. Instead, our findings align with a rich neurophysiological literature demonstrating that these rest-based improvements are the behavioral signature of a genuine, hippocampus-dependent process. For instance, they are predicted by the level of hippocampal and precuneus activity during rest[14] and are directly correlated with the rate of waking hippocampo-neocortical replay[15]. Therefore, a plausible synthesis is that micro-offline gains are a multifaceted phenomenon, reflecting a combination of both transient performance factors and true memory consolidation. Our work, by providing a direct causal link between the hippocampus and the expression of these gains, offers compelling evidence that a significant component of them is indeed a product of the brain's core memory machinery.

The ability to non-invasively induce a "high-online" learning state has profound translational potential. In neurorehabilitation settings, such as post-stroke motor recovery, where patient fatigue is a primary limiting factor for the duration and intensity of therapy[61], a TUS-based approach that maximizes learning efficiency per minute of active practice could significantly accelerate recovery. Furthermore, for populations with impaired sleep-dependent consolidation, such as older adults who show age-related declines in sleep spindles and associated memory benefits[62], the ability to shift the burden of consolidation to the active practice phase could offer a powerful therapeutic strategy. However, this

"paradoxical enhancement" must be approached with caution. The brain's default preference for offline consolidation likely serves a protective function, preventing the overwriting of existing memories through "catastrophic interference"[54]. Future research must therefore investigate the potential costs of this TUS-induced "super-learning" state, including its metabolic demands and its impact on cognitive flexibility or the stability of previously established memories.

While our behavioral results are robust, two limitations highlight the need for further research to fully elucidate the neural mechanisms underlying this effect. First, a primary limitation is the absence of concurrent neural recordings. We infer a systemic shift from a hippocampal-dependent offline pathway to a corticostriatal-dependent online pathway but did not directly measure the neural signatures of this change. Future studies combining hippocampal TUS with concurrent fMRI or EEG are therefore essential to confirm how hippocampal-cortical interactions are altered and to directly track the neural correlates of online and offline gains. Furthermore, to confirm the anatomical specificity of this mechanism, future work should include an active control stimulation site. While our personalized targeting ensures the acoustic focus is on the hippocampus, targeting a control region not thought to be involved in this process, such as the cerebellum, would provide definitive evidence that the observed shift in learning dynamics is specific to hippocampal modulation. Addressing these key neurobiological questions will be the critical next step in leveraging this powerful neuromodulatory technique.

In conclusion, our study identifies the human hippocampus as a crucial regulator of the temporal dynamics involved in motor learning. By directly inhibiting the hippocampus, we shifted the primary mechanism of skill acquisition from offline

consolidation to a more efficient online learning mode. This finding offers causal evidence for the hippocampus's role in procedural memory and, more broadly, suggests that targeted modulation of memory dynamics can optimize human performance.

Materials and Methods

Participants

A total of fifty-two healthy volunteers (32 female) participated in the study. The study comprised two experiments: a TUS validation study on motor cortex excitability and a main behavioral experiment. The validation study involved forty participants, randomly assigned to either a TUS group (N=20) or a sham group (N=20). The main behavioral experiment included forty participants, randomly assigned to either a TUS group (N=20) or a sham group (N=20). This behavioral cohort was composed of twenty-eight individuals who also participated in the validation experiment. All participants were free of medications known to alter brain excitability and reported no history of neurological or psychiatric disorders. Participants were kept blind to the specific experimental objectives until the conclusion of their involvement. A minimum washout period of five days was maintained between sessions to prevent carry-over effects. The study protocol was approved by the local Institutional Review Board (IRB), and all participants provided written informed consent prior to participation. The study was performed in accordance with the Declaration of Helsinki.

Experimental Design

The study followed a randomized, between-subject design. The main experiment involved two groups: a Hippocampal TUS group (N=20) and a Sham group (N=20). The experiment spanned two consecutive days (Fig. 1A). On Day 1, participants received either active or sham TUS stimulation immediately before engaging in a 36-trial motor sequence learning task. Approximately 24 hours later, on Day 2, participants returned for a 9-trial retention test without any further stimulation. A separate TUS validation

experiment was conducted on a cohort of 40 participants to confirm the neurophysiological effects of the stimulation parameters.

Motor Sequence Task

Participants learned a procedural motor skill task adapted from prior work (Bönstrup et al., 2019)[13]. Using their non-dominant (left) hand, they were instructed to type a five-element sequence (4-1-3-2-4) as quickly and accurately as possible. The key presses were mapped to a standard QWERTY keyboard (4=index, 3=middle, 2=ring, 1=pinky). The sequence was continuously displayed on a monitor, and an asterisk appeared after each keypress to provide immediate feedback on task execution. The experiment was conducted over two consecutive days. On Day 1, participants performed 36 training trials. On Day 2, they completed a 9-trial retention test. Each trial consisted of a 10-second practice period followed by a 10-second rest period (Fig. 1A). Participants were instructed to focus on the visually presented five-item sequence during the practice periods and to execute it as many times as possible. During the rest periods, the sequence was replaced on the screen by five "X" symbols (X-X-X-X-X), and participants were instructed to fixate on the screen while keeping their hands still. Thus, a single trial included one practice period followed by one rest period. Each participant was tested at a similar time of day on both days (±2 hours) in an attempt to control circadian variations.

Transcranial Ultrasound Stimulation (TUS)

TUS was administered using a four-element, 500 kHz spherical ultrasound transducer (Model: DPX-500-4CH-008; 64.0 mm diameter, 63.2 mm radius of curvature; Sonic Concepts). The stimulation protocol consisted of 200 ms bursts repeated at 5 Hz for a total duration of 80 seconds (400 bursts total), with each burst having a duty cycle of 10%.

For each participant, the transducer's focal depth and intensity were personalized using transcranial acoustic simulations (see "Personalized TUS Targeting" section in Results). The goal of these simulations was to precisely target the posterior hippocampus while ensuring all acoustic and thermal parameters remained well below the safety guidelines established by the FDA for diagnostic ultrasound (e.g., MI ≤ 1.9; I_{sppa} ≤ 190 W/cm²)[63]. The resulting group-averaged in situ acoustic parameters, including I_{sppa}, peak pressure, Mechanical Index (MI), and thermal dose (CEM43), are reported in the Results section.

Acoustic Measurements using a Calibrated Hydrophone. The acoustic output of the ultrasound transducer was physically characterized using a calibrated hydrophone scanning system (AIMS III; Onda Corp.) in a degassed water tank at room temperature (Fig. 1B). A hydrophone (HGL-0200; Onda Corp.) was mounted on a 3-axis positioning system, and its signal was passed through a pre-amplifier to an oscilloscope synchronized with the transducer's output. The system first located the acoustic focus by performing a 3D scan to identify the point of maximum peak pressure. Following localization, a high-resolution one-dimensional scan was performed along the z-axis to map the axial beam profile, with the AIMS software computing all key acoustic parameters at each spatial location.

Anatomical MRI Acquisition. Prior to the TUS experiments, a high-resolution T1-weighted structural MRI was acquired for each participant using a magnetization-prepared gradient-echo (MPRAGE) sequence on a 3T Siemens Prisma scanner. The sequence yielded images with a 1 mm³ isotropic resolution (matrix size = 256 × 256 × 192; repetition time (TR) = 2300 ms; echo time (TE) = 2.28 ms; flip angle = 8°). These anatomical images served two primary purposes: (1) to generate pseudo-CT images for

514 personalized acoustic simulations and (2) for neuronavigated targeting of the
515 hippocampus with the Brainsight system (Rogue Research, Canada).

516 **Pseudo-CT Generation for Acoustic Modeling.** Accurate transcranial acoustic
517 simulation is critical for the safe and effective delivery of ultrasound energy, as it must
518 account for the absorption and refraction of the acoustic beam by the skull[64]. While CT
519 scans provide the "gold standard" for skull modeling, they involve ionizing radiation[65]. To
520 circumvent this, we generated pseudo-CT images directly from each participant's T1-
521 weighted MRI. This was achieved using an open-source, deep-learning toolbox[66], which
522 employs a pre-trained convolutional neural network (CNN) to estimate skull density and
523 geometry from anatomical MRI data. Prior to conversion, the T1-weighted images were
524 bias-corrected and brain-extracted to optimize the input for the CNN. This approach
525 enabled us to conduct precise, personalized acoustic and thermal simulations for each
526 participant without exposure to radiation.

527 **TUS Simulation**. To accurately account for the impact of individual skull morphology on
528 ultrasound wave propagation, we simulated the TUS focus using a commercial toolbox
529 (k-Plan, Brainbox, UK). The simulations were based on each participant's unique skull
530 structure, derived from the pseudo-CT images described above. Prior to simulation, the
531 pseudo-CTs were calibrated to transform Hounsfield Units (HU) into mass density
532 (threshold: 300 HU; limit: 2000 HU) and then segmented into three material types: skull
533 bone (>1,150 kg/m ^{3}), soft tissue (1,045 kg/m ^{3}), and water (996 kg/m ^{3}). For each
534 participant, the transducer's position and orientation were iteratively adjusted to ensure
535 the simulated acoustic focus was precisely positioned on the posterior hippocampus, as
536 defined by their anatomical MRI. The acoustic simulations were performed in the time

537 domain, and the final pressure amplitude and phase were extracted after the field reached
538 a steady state.

539 **Personalized TUS Targeting.** The results of the individual acoustic simulations were
540 used to guide the delivery of a personalized TUS protocol for each participant. Using a
541 neuronavigation system, the physical transducer was positioned on the participant's
542 scalp, coupled with ultrasound gel. The transducer's location, orientation, and focal depth
543 were iteratively adjusted to match the optimal parameters derived from the simulation that
544 targeted the posterior hippocampus on that individual's anatomical MRI. Once targeting
545 was confirmed, the 80-second sonication protocol was administered. The transducer's
546 position was continuously monitored and maintained throughout the sonication to ensure
547 the acoustic focus remained on target. For the sham condition, the entire neuronavigation
548 and setup procedure was identical, but no acoustic energy was delivered. To mask any
549 potential auditory signals from the transducer and maintain blinding, all participants were
550 exposed to continuous Gaussian white noise for the duration of the procedure.

551 **Data and Statistical Analyses**

552 Behavioral data were processed using custom scripts in MATLAB (The MathWorks), and
553 neurophysiological data were processed in Signal software (Cambridge Electronic
554 Design). All subsequent statistical analyses were conducted using SPSS Statistics (IBM
555 Corp.). For all parametric tests, statistical assumptions were systematically verified. The
556 assumption of normality was assessed using the Shapiro-Wilk test; when this assumption
557 was not met, a logarithmic transformation was applied to the data. For between-group
558 comparisons, homogeneity of variances was evaluated using Levene's test. For
559 repeated-measures ANOVAs, the assumption of sphericity was assessed using

560 Mauchly's test; if sphericity was violated, the degrees of freedom were corrected using
561 the Greenhouse-Geisser statistic. A significance level of $p < 0.05$ was used for all
562 analyses.

563 **Behavioral Data.** The primary measure of performance was tapping speed, quantified as
564 the inverse of the time interval (in seconds) between adjacent key presses within a
565 correctly executed sequence (keypresses/s). Performance for each trial was calculated
566 as the mean tapping speed of all correctly performed sequences within that 10-s period.
567 To dissect the within-session dynamics, we calculated trial-by-trial performance changes
568 (Deltas) based on the methodology of prior work[13]. Specifically, "micro-online
569 gains" were defined as the difference in tapping speed between the first and the last
570 correct sequence within a single practice period, isolating changes that occurred during
571 active practice. "Micro-offline gains" were defined as the difference in tapping speed
572 between the last correct sequence of one practice period and the first correct sequence
573 of the next, isolating changes across the intervening rest period. The overall learning
574 trajectory was characterized by calculating learning rates for each participant by fitting an
575 exponential function to their Day 1 performance curve. To analyze performance after the
576 initial rapid learning phase, we defined a performance plateau for each participant as the
577 average tapping speed in all trials after they had reached 95% of their total Day 1 learning.
578 Finally, overnight consolidation was quantified as the difference in tapping speed
579 between the last trial of Day 1 and the first trial of Day 2.

580 **Neurophysiological Data.** To validate the neurophysiological effect of our TUS protocol,
581 we measured changes in corticospinal excitability by recording motor-evoked potentials
582 (MEPs) elicited by transcranial magnetic stimulation (TMS). Single TMS pulses were

583 administered using a DuoMAG MP-Dual TMS system (Brainbox Ltd) with a 70 mm figure-
584 of-eight coil. The coil was positioned tangentially over the primary motor cortex (M1) hand
585 knob, with the handle pointing posteriorly and laterally at approximately a 45° angle to the
586 midline. This position was individually identified and monitored using a neuronavigation
587 system co-registered to each participant's anatomical MRI. Stimulus intensity was defined
588 as the minimum required to evoke MEPs with a peak-to-peak amplitude of >1 mV in at
589 least 5 out of 10 consecutive trials and was held constant throughout the experiment[67,68].
590 MEPs were recorded from the contralateral first dorsal interosseous (FDI) muscle using
591 disposable Ag-AgCl surface electrodes in a belly-tendon montage. The
592 electromyographic (EMG) signal was amplified, band-pass filtered (30–2000 Hz) using a
593 Neurolog System (Digitimer), and digitized at a sampling rate of 10 kHz for offline analysis
594 (CED Micro 1401). For each participant, MEPs were recorded at three time points: a
595 baseline block (24 pulses) prior to the TUS intervention, a second block (24 pulses) at 5
596 minutes post-TUS, and a final block (24 pulses) at 30 minutes post-TUS. For the TUS
597 component of this validation experiment, stimulation was delivered using a transducer
598 specifically designed for superficial cortical targets (Model: CTX-500-4CH-082; Sonic
599 Concepts). The average MEP amplitude from each block was used for statistical analysis.

600 **Statistical Analysis.** For the TUS validation experiment, a 2 (Group: TUS, Sham) × 3
601 (Time: Baseline, 5 min, 30 min) mixed-model ANOVA was performed on the MEP
602 amplitudes, with post-hoc tests used to analyze significant interactions. For the main
603 behavioral experiment, a series of t-tests and correlations were used. The contribution of
604 micro-online and micro-offline gains to learning within each group was assessed using
605 one-sample t-tests against a test value of zero. Direct comparisons of all primary

behavioral metrics between the TUS and sham groups—including summed micro-gains, learning rates, performance during the plateau phase, and overnight consolidation—were performed using independent-samples t-tests. Finally, relationships between variables, such as the trade-off between online and offline gains and the prediction of overnight consolidation from Day 1 learning dynamics, were assessed using Pearson's correlation coefficient (r).

References

1. Dayan, E., & Cohen, L. G. (2011). Neuroplasticity subserving motor skill learning. Neuron, 72(3), 443-454.
2. Krakauer, J. W., Hadjiosif, A. M., Xu, J., Wong, A. L., & Haith, A. M. (2019). Motor learning. Comprehensive Physiology, 9(2), 613-663.
3. Robertson, E. M., Pascual-Leone, A., & Miall, R. C. (2004). Current concepts in procedural consolidation. Nature Reviews Neuroscience, 5(7), 576-582.
4. Dudai, Y. (2004). The neurobiology of consolidations, or, how stable is the engram?. Annual Review of Psychology, 55, 51-86.
5. Wang, Y., Huynh, A. T., Bao, S., Buchanan, J. J., Wright, D. L., & Lei, Y. (2024). Memory consolidation of sequence learning and dynamic adaptation during wakefulness. Cerebral Cortex, 34(2).
6. Bao, S., Wang, J., Wright, D. L., Buchanan, J. J., & Lei, Y. (2022). The decay and consolidation of effector-independent motor memories. Scientific Reports, 12(1), 3131.
7. Frankland, P. W., & Bontempi, B. (2005). The organization of recent and remote memories. Nature Reviews Neuroscience, 6(2), 119-130.
8. Antony, J. W., Gobel, E. W., O'Hare, J. K., Reber, P. J., & Paller, K. A. (2012). Cued memory reactivation during sleep leads to specific task improvement. Nature Neuroscience, 15(3), 478-482.
9. Walker, M. P., Brakefield, T., Morgan, A., Hobson, J. A., & Stickgold, R. (2002). Practice with sleep makes perfect: sleep-dependent motor skill learning. Neuron, 35(1), 205-211.
10. Diekelmann, S., & Born, J. (2010). The memory function of sleep. Nature Reviews Neuroscience, 11(2), 114-126.
11. Rasch, B., & Born, J. (2013). About sleep's role in memory. Physiological Reviews, 93(2), 681-766.
12. Dudai, Y., & Eisenberg, M. (2004). Rites of passage of the engram: reconsolidation and the lingering consolidation hypothesis. Neuron, 44(1), 93-100.
13. Bönstrup, M., Iturrate, I., Thompson, R., Cruciani, G., Censor, N., & Cohen, L. G. (2019). A rapid form of offline consolidation in skill learning. Current Biology, 29(8), 1346-1351.
14. Jacobacci, F., Armony, J. L., Yeffal, A., Lerner, G., Amaro Jr, E., Jovicich, J., ... & Della-Maggiore, V. (2020). Rapid hippocampal plasticity supports motor sequence learning. Proceedings of the National Academy of Sciences, 117(38), 23898-23903.
15. Buch, E. R., Claudino, L., Quentin, R., Bönstrup, M., & Cohen, L. G. (2021). Consolidation of human skill linked to waking hippocampo-neocortical replay. Cell Reports, 35(10), 109193.
16. Gann, M. A., Dolfen, N., King, B. R., Robertson, E. M., & Albouy, G. (2023). Prefrontal stimulation as a tool to disrupt hippocampal and striatal reactivations underlying fast motor memory consolidation. Brain Stimulation, 16(5), 1336-1345.
17. Mylonas, D., Schapiro, A. C., Verfaellie, M., Baxter, B., Vangel, M., Stickgold, R., & Manoach, D. S. (2024). Maintenance of Procedural Motor Memory across Brief Rest Periods Requires the Hippocampus. The Journal of Neuroscience, 44(14).
18. Polanía, R., Nitsche, M. A., & Ruff, C. C. (2018). Studying and modifying brain function

with non-invasive brain stimulation. Nature Neuroscience, 21(2), 174-187.
19. Thielscher, A., & Kammer, T. (2004). Electric field properties of two commercial figure-8 coils in TMS: calculation of focality and efficiency. Clinical Neurophysiology, 115(7), 1697-1708.
20. Bestmann, S., & Walsh, V. (2017). Transcranial magnetic stimulation of human cortex. Current Biology, 27(22), R1228-R1232.
21. Bikson, M., Grossman, P., Thomas, C., Zannou, A. L., Jiang, J., Adnan, T., ... & Woods, A. J. (2016). Safety of transcranial direct current stimulation: evidence based update 2016. Brain Stimulation, 9(5), 641-661.
22. Lozano, A. M., & Lipsman, N. (2013). Probing and regulating dysfunctional circuits using deep brain stimulation. Neuron, 77(3), 406-424.
23. Suthana, N., Haneef, Z., Stern, J., Mukamel, R., Behnke, E., Knowlton, B., & Fried, I. (2012). Memory enhancement and deep-brain stimulation of the entorhinal area. New England Journal of Medicine, 366(6), 502-510.
24. Fenoy, A. J., & Schiess, M. C. (2017). Deep brain stimulation of the fornix for global amnesia. Neurosurgery Clinics, 28(4), 593-601.
25. Hamani, C., McAndrews, M. P., Cohn, M., Oh, M., Zumsteg, D., Shapiro, C. M., ... & Lozano, A. M. (2008). Memory enhancement induced by hypothalamic/fornix deep brain stimulation. Annals of Neurology, 63(1), 119-123.
26. Beric, A. (2009). Complications of deep brain stimulation surgery. Movement Disorders, 24(S2), S339-S343.
27. Fenoy, A. J., Simpson Jr, R. K., & Schiess, M. C. (2016). The safety of deep brain stimulation: a review of the literature. Journal of Neurosurgery, 124(3), 775-785.
28. Legon, W., Sato, T. F., Opitz, A., Mueller, J., Barbour, A., Williams, A., & Tyler, W. J. (2014). Transcranial focused ultrasound modulates the activity of primary somatosensory cortex in humans. Nature Neuroscience, 17(2), 322-329.
29. Tyler, W. J., Tufail, Y., Finsterwald, M., Tauchmann, M. L., Olson, E. J., & Majestic, C. (2008). Remote excitation of neuronal circuits using low-intensity, low-frequency ultrasound. PloS one, 3(10), e3511.
30. Fomenko, A., Neudorfer, C., Dallapiazza, R. F., Kalia, S. K., & Lozano, A. M. (2018). Low-intensity ultrasound neuromodulation: an overview of mechanisms and emerging human applications. Brain Stimulation, 11(6), 1209-1217.
31. Blackmore, J., Shrivastava, S., Sallet, J., Butler, C. R., & Cleveland, R. O. (2019). Ultrasound neuromodulation: a review of results, mechanisms and safety. Ultrasound in Medicine & Biology, 45(7), 1509-1536.
32. Yoo, S. S., Bystritsky, A., Lee, J. H., Zhang, Y., Fischer, K., Min, B. K., ... & Jolesz, F. A. (2011). Focused ultrasound modulates region-specific brain activity. Neuroimage, 56(3), 1267-1275.
33. Na, Y., Paeng, D. G., & Yoo, Y. (2020). Mechanosensitive ion channels and their role in ultrasonic neuromodulation. Journal of Medical and Biological Engineering, 40(4), 487-498.
34. Zeng, K., Darmani, G., Fomenko, A., Xia, X., Tran, S., Nankoo, J. F., ... & Chen, R. (2022). Induction of human motor cortex plasticity by theta burst transcranial ultrasound stimulation. Annals of Neurology, 91(2), 238-252.
35. Tufail, Y., Matyushov, A., Baldwin, N., Tauchmann, M. L., Georges, J., Yoshihiro, A., ... & Tyler, W. J. (2010). Transcranial pulsed ultrasound stimulates intact brain

circuits. Neuron, 66(5), 681-694.
36. King, R. L., Brown, J. R., Newsome, W. T., & Pauly, K. B. (2013). Effective parameters for ultrasound-induced in vivo neurostimulation. Ultrasound in medicine & biology, 39(2), 312-331.
37. Folloni, D., Verhagen, L., Mars, R. B., Fouragnan, E., Constans, C., Aubry, J. F., ... & Sallet, J. (2019). Manipulation of subcortical and deep cortical activity in the primate brain using transcranial focused ultrasound stimulation. Neuron, 101(6), 1109-1116.
38. Legon, W., Ai, L., Bansal, P., & Mueller, J. K. (2018). Neuromodulation with single-element transcranial focused ultrasound in human thalamus. Human Brain Mapping, 39(5), 1995-2006.
39. Bao, S., Kim, H., Shettigar, N. B., Li, Y., & Lei, Y. (2024). Personalized depth-specific neuromodulation of the human primary motor cortex via ultrasound. The Journal of Physiology, 602(5), 933-948.
40. Hou, L., & Lei, Y. (2025). Spinal cord ultrasound stimulation modulates corticospinal excitability in humans. Brain Stimulation, 18(4), 1116-1130.
41. Pasquinelli, C., Hanson, L. G., Siebner, H. R., Lee, H. J., & Thielscher, A. (2019). Safety of transcranial focused ultrasound stimulation: a systematic review of the state of knowledge from both human and animal studies. Brain Stimulation, 12(6), 1367-1380.
42. Legon, W., & Tyler, W. J. (2017). Transcranial focused ultrasound for neuromodulation: A review of the technology and its applications. Brain Stimulation, 10(6), 998-1006.
43. Monti, M. M., Schnakers, C., Korb, A. S., Bystritsky, A., & Vespa, P. M. (2016). Non-invasive ultrasonic thalamic stimulation in disorders of consciousness after severe brain injury: a first-in-man report. Brain Stimulation, 9(6), 940-941.
44. Cain, J. A., Visagan, S., Johnson, M. A., Crone, J., Blades, R., Spivak, N. M., ... & Monti, M. M. (2021). Real time and delayed effects of subcortical low intensity focused ultrasound. Scientific Reports, 11(1), 1-14.
45. Sanguinetti, J. L., Hameroff, S., Smith, E. E., Sato, T., Daft, C., Tyler, W. J., & Allen, J. J. (2020). Transcranial focused ultrasound to the right prefrontal cortex improves mood and alters functional connectivity in humans. Frontiers in Human Neuroscience, 14, 52.
46. Lee, W., Kim, H. C., Jung, Y., Chung, Y. A., Song, I. U., Lee, J. H., & Yoo, S. S. (2016). Transcranial focused ultrasound stimulation of human primary visual cortex. Scientific Reports, 6(1), 1-8.
47. Fomenko, A., Chen, K. H. S., Nankoo, J. F., Saravanamuttu, J., Wang, Y., El-Baba, M., ... & Chen, R. (2020). Systematic examination of low-intensity ultrasound parameters on human motor cortex excitability and behavior. Elife, 9, e54497.
48. Eguchi, K., Shindo, T., Ito, K., Ogata, T., Kurosawa, R., Kagaya, Y., ... & Shimokawa, H. (2018). Whole-brain low-intensity pulsed ultrasound therapy markedly improves cognitive dysfunctions in mouse models of dementia-Crucial roles of endothelial nitric oxide synthase. Brain Stimulation, 11(5), 959-973.
49. Jung, J., Atkinson-Clement, C., Kaiser, M. *et al.* Transcranial focused ultrasound stimulation enhances semantic memory by modulating brain morphology, neurochemistry and neural dynamics. Nat Commun (2026).
50. Poldrack, R. A., & Packard, M. G. (2003). Competition among multiple memory

systems: converging evidence from animal and human brain studies. Neuropsychologia, 41(3), 245–251.

51. Eckart, M. T., Huelse-Matia, M. C., & Schwarting, R. K. W. (2012). Dorsal hippocampal lesions boost performance in the rat sequential reaction time task. Hippocampus, 22(5), 1202–1214.
52. Reber, P. J., & Squire, L. R. (1998). Encapsulation of implicit and explicit memory in sequence learning. Journal of Cognitive Neuroscience, 10(2), 248–263.
53. Foerde, K., Knowlton, B. J., & Poldrack, R. A. (2006). Modulation of competing memory systems by distraction. Proceedings of the National Academy of Sciences, 103(31), 11778–11783.
54. McClelland, J. L., McNaughton, B. L., & O'Reilly, R. C. (1995). Why there are complementary learning systems in the hippocampus and neocortex: insights from the successes and failures of connectionist models of learning and memory. Psychological Review, 102(3), 419–457.
55. Packard, M. G., & Knowlton, B. J. (2002). Learning and memory functions of the basal ganglia. Annual Review of Neuroscience, 25(1), 563–593.
56. Doyon, J., Korman, M., Morin, A., Dostie, V., Hadj Tahar, A., Benali, H., Karni, A., Ungerleider, L. G., & Carrier, J. (2009). Contribution of night and day sleep vs. simple passage of time to the consolidation of motor sequence and visuomotor adaptation learning. Experimental Brain Research, 195(1), 15–26.
57. Mednick, S. C., Cai, D. J., Shuman, T., Anagnostaras, S., & Wixted, J. T. (2011). An opportunistic theory of cellular and systems consolidation. Trends in Neurosciences, 34(10), 504–514.
58. Poldrack, R. A., & Packard, M. G. (2003). Competition among multiple memory systems: converging evidence from animal and human brain studies. Neuropsychologia, 41(3), 245–251.
59. White, N. M., & McDonald, R. J. (2002). Multiple parallel memory systems in the brain of the rat. Neurobiology of Learning and Memory, 77(2), 125–184.
60. Das, A., Karagiorgis, A., Diedrichsen, J., Stenner, M. P., & Azañón, E. (2025). Micro-offline gains do not reflect offline learning during early motor skill acquisition in humans. PNAS, 122(44), e2509233122.
61. Mead, G., Lynch, J., Greig, C., Young, A., Lewis, S., & Sharpe, M. (2012). Evaluation of a complex intervention for post-stroke fatigue: a pilot randomized controlled trial. Journal of Neurology, Neurosurgery & Psychiatry, 83(9), 923–928.
62. Mander, B. A., Winer, J. R., & Walker, M. P. (2017). Sleep and human aging. Neuron, 94(1), 19–36.
63. Food, U. (2019). D. Administration, Marketing clearance of diagnostic ultrasound systems and transducers: Guidance for industry and Food and Drug Administration staff. *Center for Devices and Radiological Health, US Food and Drug Administration, Rockville, MD, Tech. Rep*.
64. Pinton, G. F., Trahey, G. E., & Dahl, J. J. (2011). Sources of image degradation in fundamental and harmonic ultrasound imaging using nonlinear, full-wave simulations. *IEEE transactions on ultrasonics, ferroelectrics, and frequency control*, *58*(4), 754-765.
65. Aubry, J. F., Tanter, M., Pernot, M., Thomas, J. L., & Fink, M. (2003). Experimental demonstration of noninvasive transskull adaptive focusing based on prior computed

tomography scans. *The Journal of the Acoustical Society of America*, *113*(1), 84-93.
66. Yaakub, S. N., White, T. A., Kerfoot, E., Verhagen, L., Hammers, A., & Fouragnan, E. F. (2023). Pseudo-CTs from T1-weighted MRI for planning of low-intensity transcranial focused ultrasound neuromodulation: An open-source tool. *Brain Stimulation: Basic, Translational, and Clinical Research in Neuromodulation*, *16*(1), 75-78.
67. Bao, S., & Lei, Y. (2025). Modulating motor cortex plasticity via cortical and peripheral somatosensory stimulation. *Journal of Neurophysiology*, *133*(6), 1955-1966.
68. Bao, S., Wang, Y., Escalante, Y. R., Li, Y., & Lei, Y. (2024). Modulation of motor cortical inhibition and facilitation by touch sensation from the glabrous skin of the human hand. *Eneuro*, *11*(3).

Figure legends

Figure 1. Experimental Design and Acoustic Characterization. (**A**) Schematic of the experimental design. Participants were assigned to either a Hippocampal Transcranial Ultrasound Stimulation (TUS) or a Sham group and performed a motor sequence learning task over two days. On Day 1, participants completed 36 trials immediately following the intervention. On Day 2, a 9-trial retention test was administered without any stimulation. Each trial consisted of a 10-s practice period, during which participants typed the five-element sequence (4-1-3-2-4), followed by a 10-s rest period. (**B**) Schematic of the hydrophone measurement setup used for acoustic characterization, consisting of the ultrasound transducer and a hydrophone submerged in a tank of degassed water and controlled by a 3-axis motor system. (**C**) Validation of the acoustic simulation. The plot shows the axial pressure profiles from the physical hydrophone (Measurement, red) and the computational (Simulation, blue), demonstrating excellent concordance. The -3 dB (Full-Width at Half-Maximum, FWHM) and -6 dB axial widths are indicated by dashed lines. (**D**) Characterization of the simulated three-dimensional pressure field. Middle panel: A 2D rendering of the acoustic pressure field along the beam's central trajectory (z-axis) demonstrates a highly collimated acoustic wave. Top right panel: The pressure map at the focal plane shows a well-defined, circular focal spot. Bottom right panel: The lateral pressure profile shows the FWHM (-3 dB width) and -6 dB width of the focal spot.

Figure 2. Personalized TUS Targeting and Physiological Validation. (**A**) Personalized TUS targeting pipeline. Top row: A high-resolution T1-weighted anatomical magnetic resonance imaging (MRI) was acquired for each participant. Middle

862 row: The T1 image was used to generate a subject-specific pseudo-computed
863 tomography (CT), providing a model of skull density and morphology for acoustic
864 simulation. Bottom row: The simulation, incorporating the individual's skull properties,
865 was used to map the transcranial pressure field and confirm that the acoustic focus was
866 precisely steered onto the individually localized hippocampus. The color bar indicates
867 pressure in megapascals (MPa). (**B**) Representative motor-evoked potential (MEP)
868 waveforms from a single participant in the TUS validation experiment, recorded at
869 baseline, 5 minutes, and 30 minutes post-stimulation over the primary motor cortex (M1).
870 (**C**) Group data for the active TUS condition (N=20). Individual participant data are shown
871 as connected lines, representing the change in MEP amplitude from baseline to 5 and 30
872 minutes post-stimulation. Post-hoc tests show a significant reduction in MEP amplitude
873 at both time points compared to baseline. (**D**) Group data for the sham stimulation
874 condition (N=20). No significant changes in MEP amplitude from baseline were observed
875 at either post-stimulation time point.
876
877 **Figure 3. Hippocampal TUS Alters the Dynamics of Rapid Memory Consolidation**
878 **on Day 1.** (**A**) Tapping speed (keypresses/s ± SEM) for the sham group across the 36
879 trials of Day 1. Magnified view of a single trial, illustrating the definition of micro-online
880 (within-practice) and micro-offline (across-rest) changes. (**B**) Trial-wise performance
881 changes (Deltas) for the sham group. Micro-offline gains (red) are consistently positive,
882 while micro-online gains (blue) fluctuate around zero. Shaded areas represent ± SEM.
883 (**C**) Sum of Deltas for the sham group. Total micro-offline gains were significantly greater
884 than zero, while total micro-online gains were not, indicating that learning was driven by

offline consolidation. (**D**) Tapping speed (keypresses/s ± SEM) for the hippocampal TUS group across the 36 trials of Day 1. (**E**) Trial-wise performance changes (Deltas) for the TUS group. The pattern is reversed: micro-online gains (blue) are now consistently positive, while micro-offline gains (red) are abolished. (**F**) Sum of Deltas for the TUS group. Total micro-online gains were significantly greater than zero, while total micro-offline gains were not, indicating a shift to online, practice-based learning. (**G**) Direct comparison of the summed gains between groups. The TUS group showed significantly greater micro-online gains, while the sham group showed significantly greater micro-offline gains. (**H**) Correlation between summed micro-online and micro-offline gains for the sham (gray) and TUS (orange) groups. A strong negative correlation was observed in both groups, indicating a conserved trade-off. TUS shifted participants from a "low-online/high-offline" to a "high-online/low-offline" regime. In all box plots, the central line indicates the median, the box edges represent the 25th and 75th percentiles, and the whiskers extend to the most extreme data points not considered outliers.

Figure 4. Hippocampal TUS Boosts Initial Performance and Overcomes Learning Plateaus. (**A**) Group-averaged learning curves (mean ± SEM) for the sham (gray) and hippocampal TUS (orange) groups on Day 1. Dashed vertical lines indicate the average trial number at which each group reached 95% of their total Day 1 learning, marking the onset of the performance plateau. (**B**) Comparison of learning rates. The sham group exhibited a significantly faster learning rate than the TUS group. (**C**) Average tapping speed during the performance plateau phase. The TUS group performed significantly better than the sham group during this phase. In all box plots, the central line indicates

908 the median, the box edges represent the 25th and 75th percentiles, and the whiskers
909 extend to the most extreme data points not considered outliers.
910
911 **Figure 5. Altered Learning Dynamics and Superior Performance Persist 24 Hours**
912 **Later.** (**A**) Tapping speed (keypresses/s ± SEM) for the sham group across the 9 retention
913 trials on Day 2. (**B**) Trial-wise performance changes (Deltas) for the sham group on Day
914 2. (**C**) Sum of Deltas for the sham group on Day 2. Neither micro-online nor micro-offline
915 gains were significantly different from zero, indicating performance had stabilized.
916 (**D**) Tapping speed (keypresses/s ± SEM) for the hippocampal TUS group on Day 2.
917 (**E**) Trial-wise performance changes (Deltas) for the TUS group on Day 2. Micro-online
918 gains remain positive, while micro-offline gains are now negative. (**F**) Sum of Deltas for
919 the TUS group on Day 2. Relearning was driven by significant micro-online gains,
920 accompanied by a significant decay in performance during rest periods (micro-offline
921 gains < 0). (**G**) Group-averaged learning curves on Day 2. The TUS group maintained a
922 significantly higher overall tapping speed throughout the retention session.
923 (**H**) Comparison of summed micro-online gains on Day 2. The TUS group showed
924 significantly greater micro-online gains than the sham group. (**I**) Comparison of summed
925 micro-offline gains on Day 2. The sham group showed significantly greater micro-offline
926 gains than the TUS group. In all box plots, the central line indicates the median, the box
927 edges represent the 25th and 75th percentiles, and the whiskers extend to the most
928 extreme data points not considered outliers.
929
930 **Figure 6. Hippocampal TUS Decouples Within-Session Learning from Overnight**

Consolidation. (**A**) Performance change across the overnight interval for the sham (gray) and TUS (orange) groups. Performance is shown for the last trial of Day 1 and the first trial of Day 2. (**B**) Total overnight gains for each group. There was no significant net change in performance overnight for either group, nor was there a significant difference between them. (**C, D**) Correlation between Day 1 learning dynamics and overnight gains in the sham group. Overnight gains were significantly negatively correlated with the sum of micro-online gains (C) and significantly positively correlated with the sum of micro-offline gains (D). (**E, F**) Correlation between Day 1 learning dynamics and overnight gains in the TUS group. The predictive relationship was completely abolished; neither micro-online gains (E) nor micro-offline gains (F) showed any significant correlation with overnight gains. Shaded areas in correlation plots represent the 95% confidence interval of the linear fit. In the box plot, the central line indicates the median, the box edges represent the 25th and 75th percentiles, and the whiskers extend to the most extreme data points not considered outliers.

Figure 1

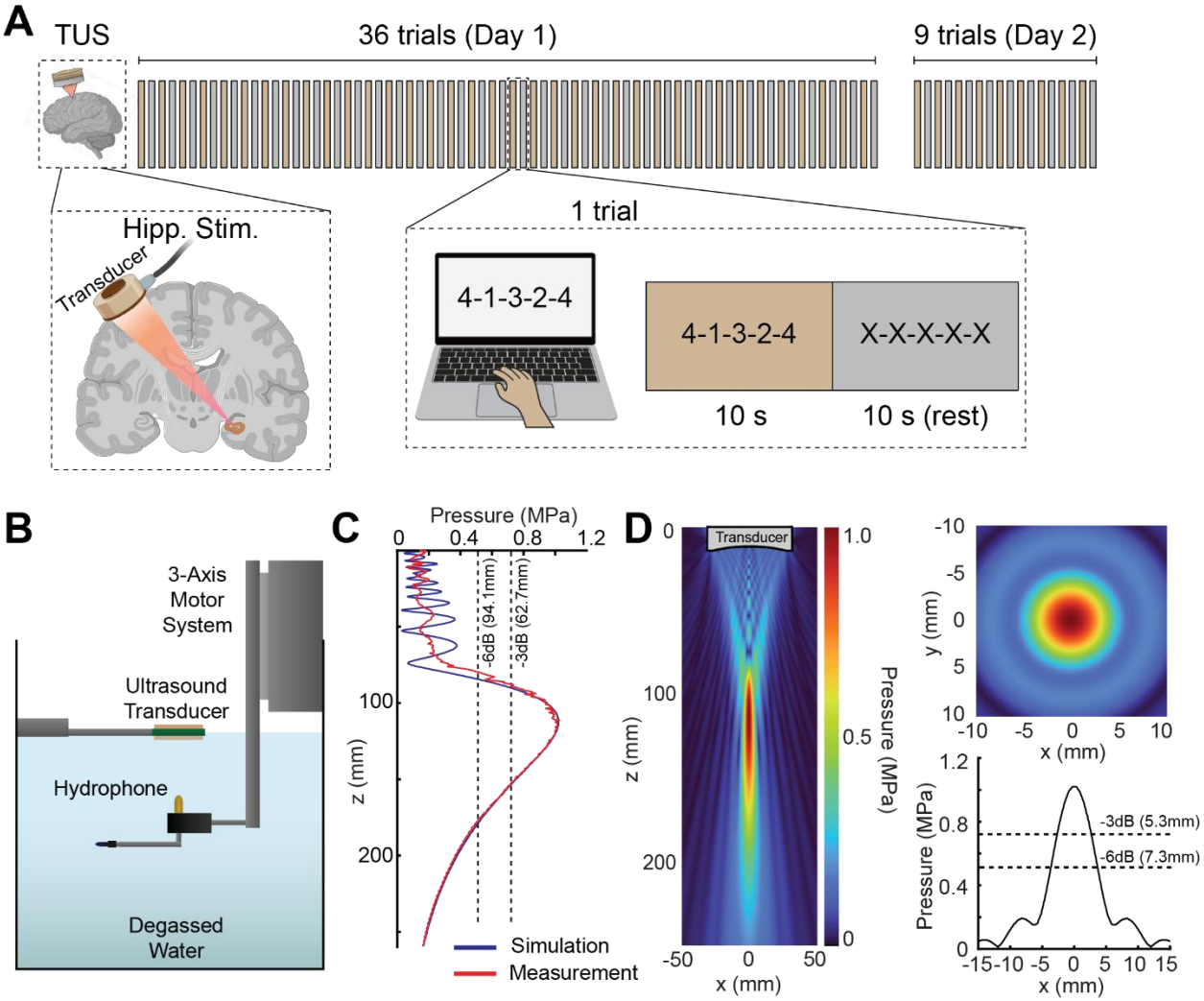
A
TUS
36 trials (Day 1)
9 trials (Day 2)
Hipp. Stim.
Transducer
1 trial
4-1-3-2-4
4-1-3-2-4
X-X-X-X-X
10 s
10 s (rest)
B
3-Axis Motor System
Ultrasound Transducer
Hydrophone
Degassed Water
C
Pressure (MPa)
0
0.4
0.8
1.2
-6dB (94.1mm)
-3dB (62.7mm)
z (mm)
100
200
Simulation
Measurement
D
Transducer
z (mm)
x (mm)
Pressure (MPa)
1.0
0.5
0
y (mm)
-3dB (5.3mm)
-6dB (7.3mm)

Figure 2

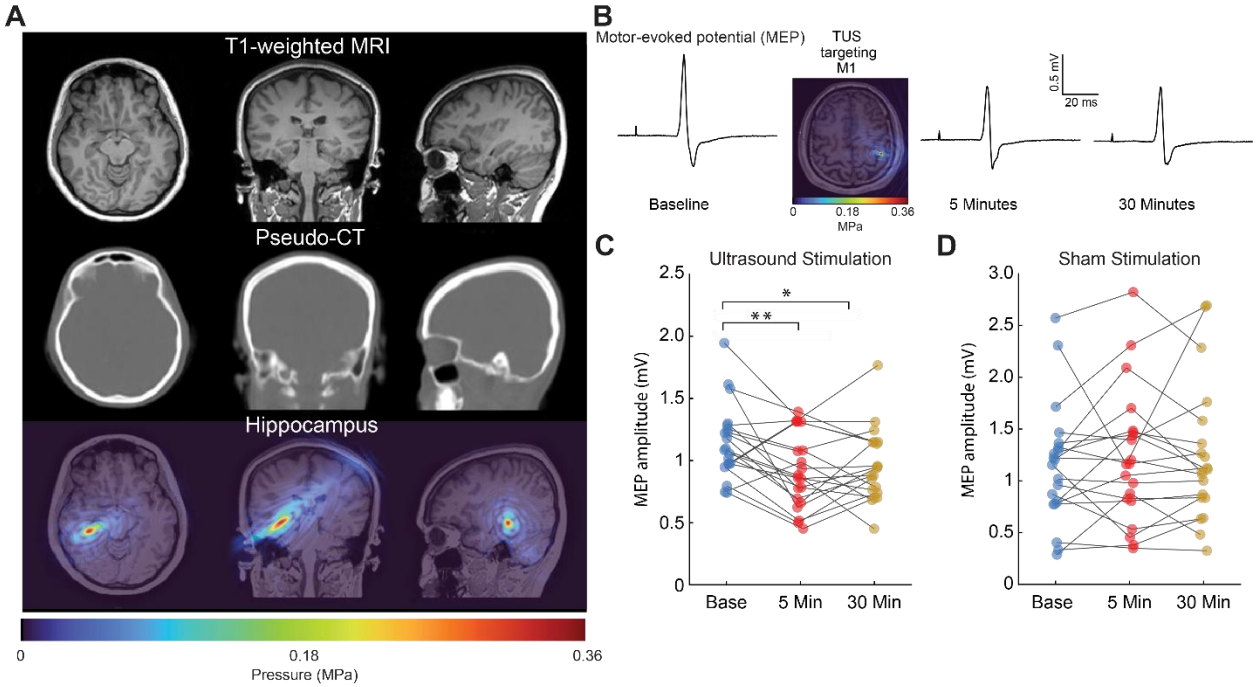
A
T1-weighted MRI
Pseudo-CT
Hippocampus
0
0.18
0.36
Pressure (MPa)
B
Motor-evoked potential (MEP)
TUS targeting M1
0.5 mV
20 ms
Baseline
0
0.18
0.36
MPa
5 Minutes
30 Minutes
C
Ultrasound Stimulation
MEP amplitude (mV)
Base
5 Min
30 Min
D
Sham Stimulation
MEP amplitude (mV)
Base
5 Min
30 Min

Figure 3

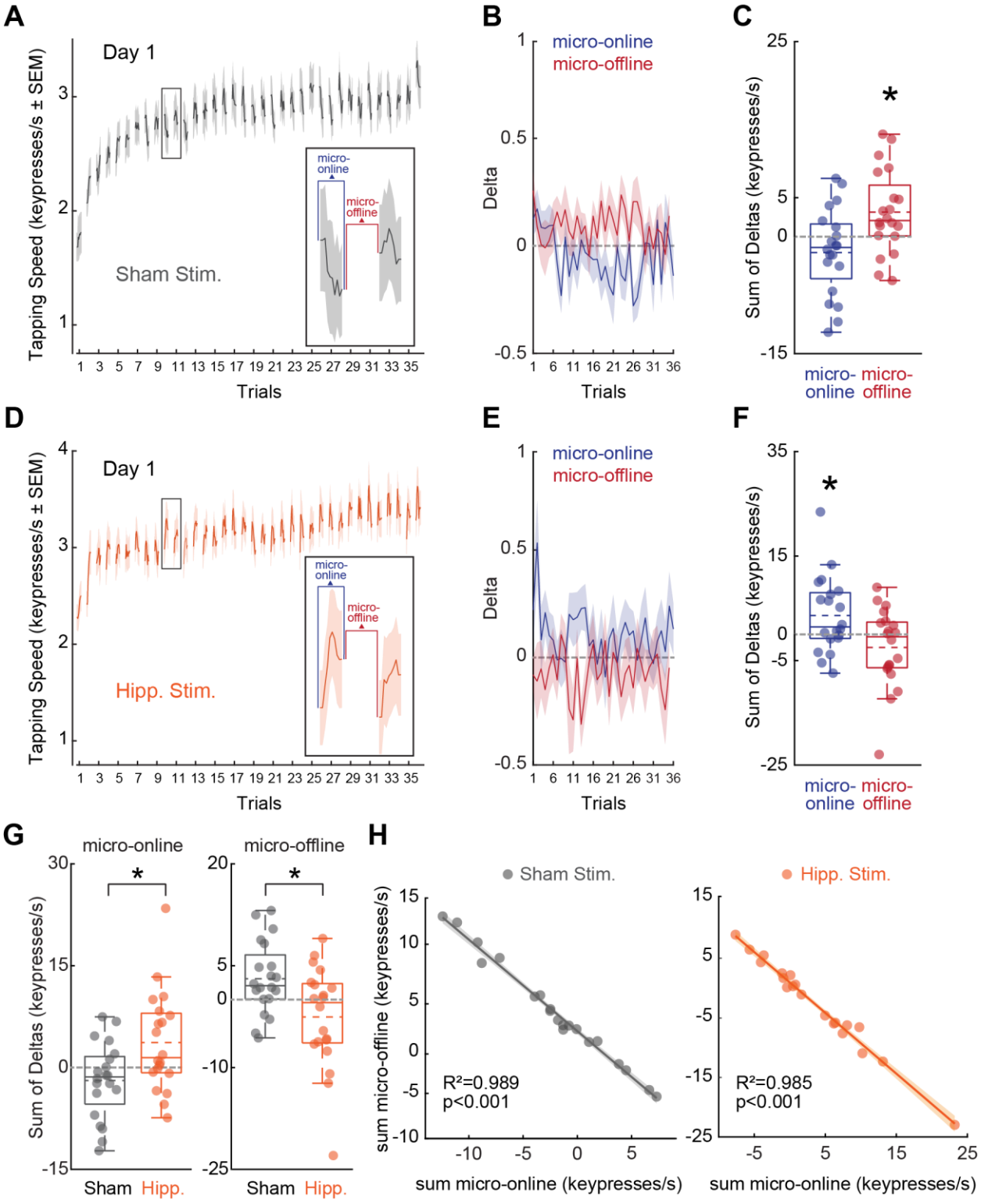
A
Day 1
Tapping Speed (keypresses/s ± SEM)
Sham Stim.
micro-online
micro-offline
Trials
B
micro-online
micro-offline
Delta
Trials
C
Sum of Deltas (keypresses/s)
micro-online
micro-offline
D
Day 1
Tapping Speed (keypresses/s ± SEM)
Hipp. Stim.
micro-online
micro-offline
Trials
E
micro-online
micro-offline
Delta
Trials
F
Sum of Deltas (keypresses/s)
micro-online
micro-offline
G
micro-online
micro-offline
Sum of Deltas (keypresses/s)
Sham
Hipp.
H
Sham Stim.
Hipp. Stim.
sum micro-offline (keypresses/s)
R²=0.989
p<0.001
R²=0.985
p<0.001
sum micro-online (keypresses/s)

Figure 4

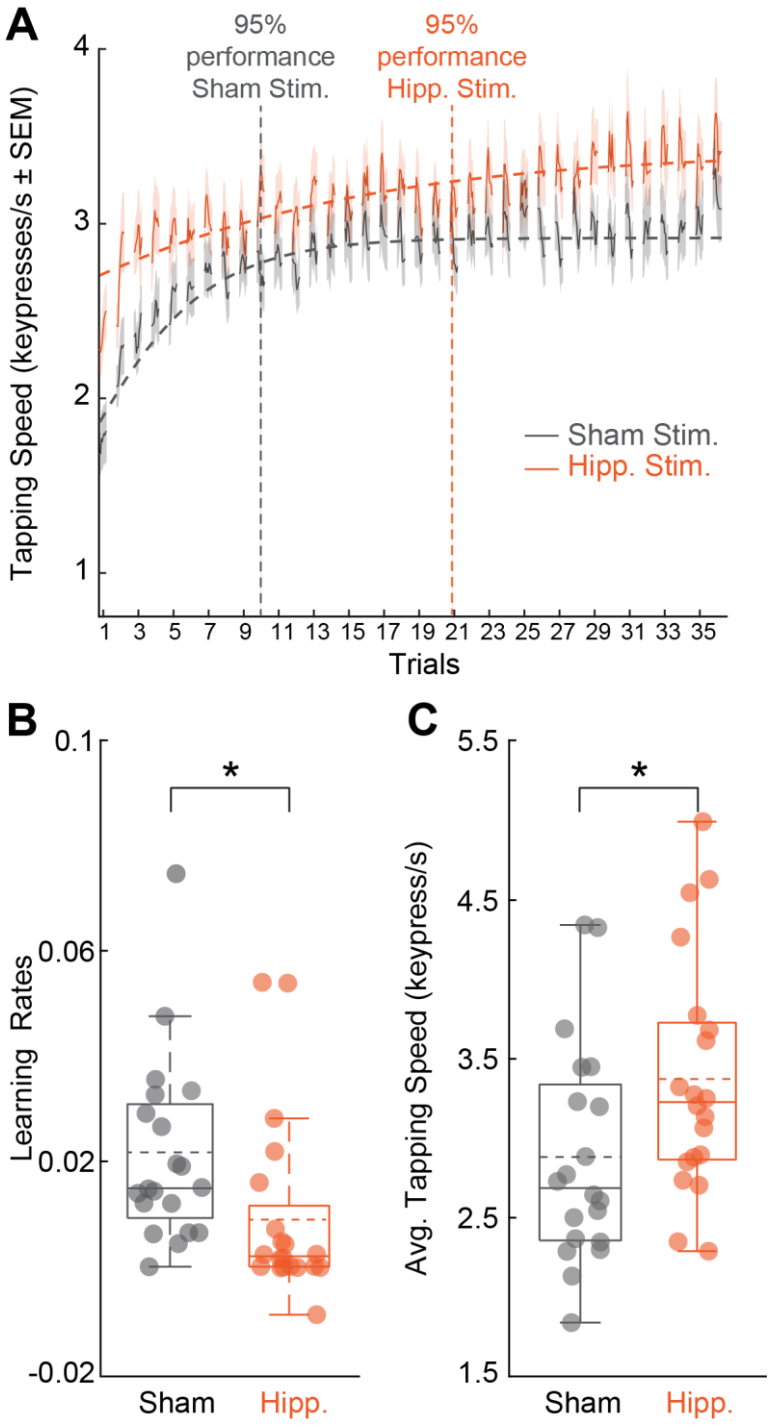
A
95% performance Sham Stim.
95% performance Hipp. Stim.
Tapping Speed (keypresses/s ± SEM)
Sham Stim.
Hipp. Stim.
Trials
B
Learning Rates
Sham
Hipp.
C
Avg. Tapping Speed (keypress/s)
Sham
Hipp.

Figure 5

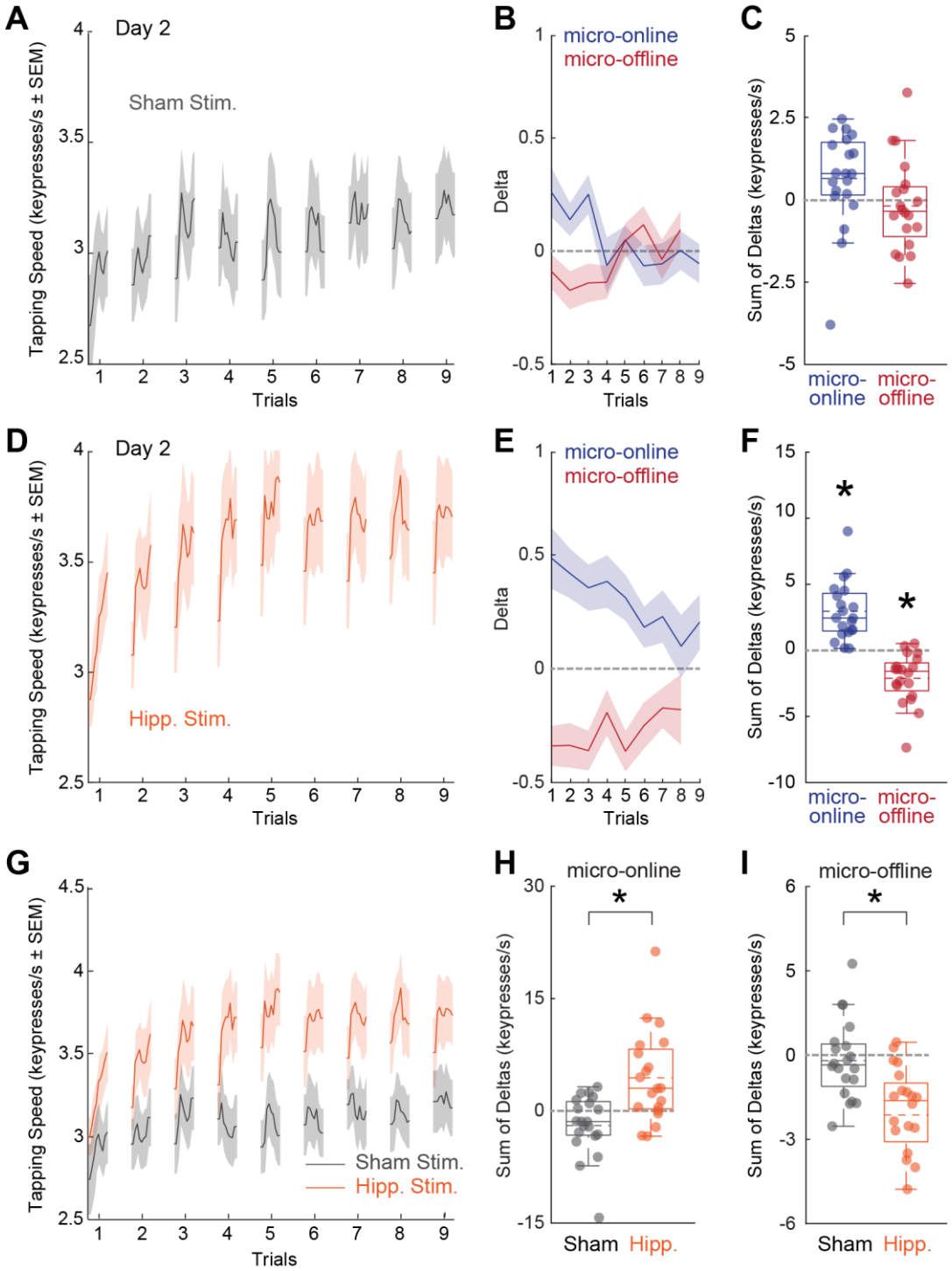
A
Day 2
Sham Stim.
Tapping Speed (keypresses/s ± SEM)
Trials
B
micro-online
micro-offline
Delta
Trials
C
Sum of Deltas (keypresses/s)
micro-online
micro-offline
D
Day 2
Hipp. Stim.
Tapping Speed (keypresses/s ± SEM)
Trials
E
micro-online
micro-offline
Delta
Trials
F
Sum of Deltas (keypresses/s)
micro-online
micro-offline
G
Tapping Speed (keypresses/s ± SEM)
Sham Stim.
Hipp. Stim.
Trials
H
micro-online
Sum of Deltas (keypresses/s)
Sham
Hipp.
I
micro-offline
Sum of Deltas (keypresses/s)
Sham
Hipp.

Figure 6

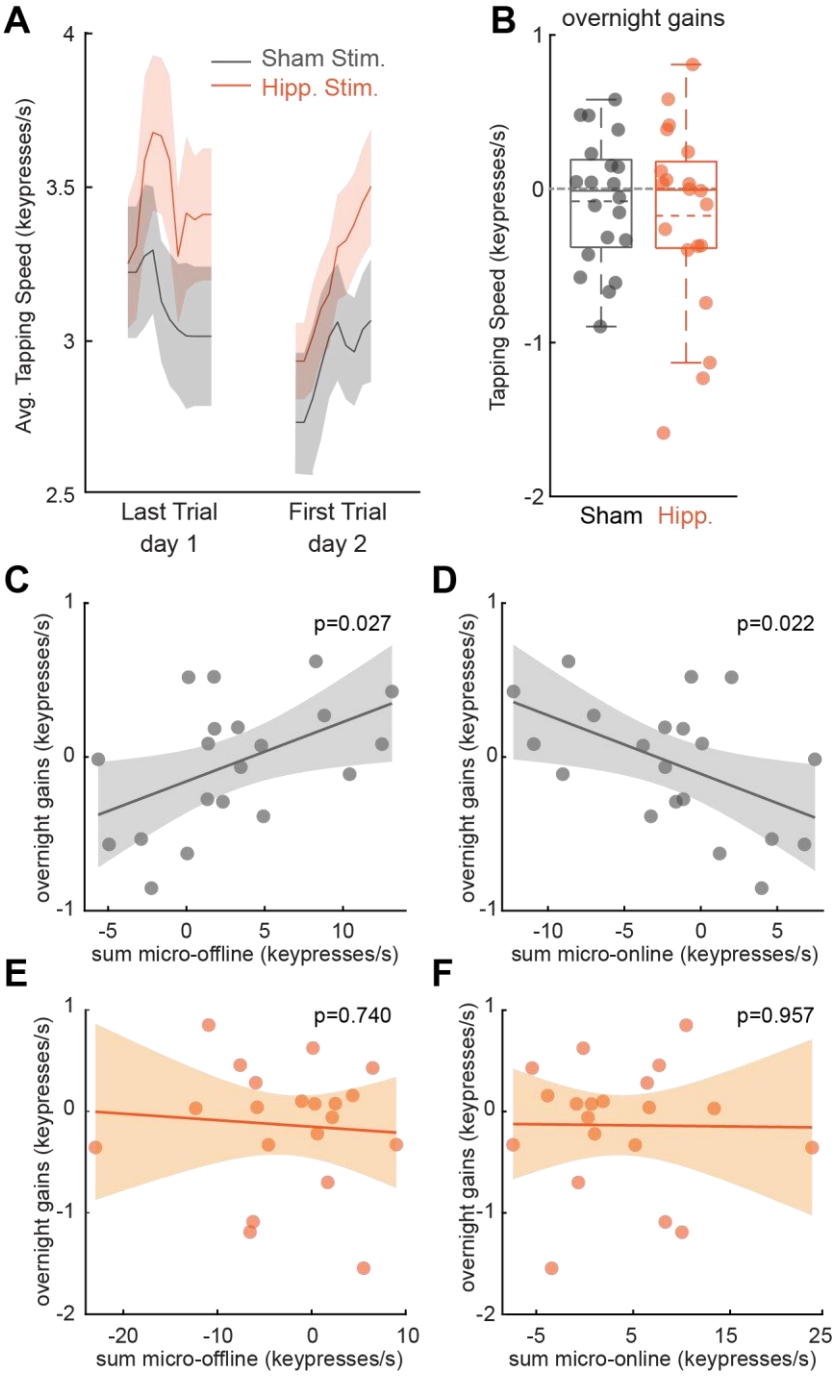
A
Sham Stim.
Hipp. Stim.
Avg. Tapping Speed (keypresses/s)
4
3.5
3
2.5
Last Trial
day 1
First Trial
day 2
B
overnight gains
Tapping Speed (keypresses/s)
1
0
-1
-2
Sham
Hipp.
C
p=0.027
overnight gains (keypresses/s)
sum micro-offline (keypresses/s)
D
p=0.022
overnight gains (keypresses/s)
sum micro-online (keypresses/s)
E
p=0.740
overnight gains (keypresses/s)
sum micro-offline (keypresses/s)
F
p=0.957
overnight gains (keypresses/s)
sum micro-online (keypresses/s)